Inorg. Chem. **1994,** *33,* 4002–4008

Coordination Characteristics of Divalent Tetrahedral (T_d and D_{2d}) Tetrahalometalate Anions of 3d Elements and Solid-State 18C6 Reorientations

Nicolette S. Fender, Shawnette S. Finegan, Dionne Miller, Maureen Mitchell, and Ishenkumba A. Kahwa*

Department of Chemistry, University of the West Indies, Mona, Kingston 7, Jamaica

Frank R. Fronczek

Department of Chemistry, Louisiana State University, Baton Rouge, Louisiana 70803

Received September 29, 1993⊛

The MX_4^{2-} compounds (M = 3d element, X = halogen) are good ligands for $[A18C6]^{n+}$ cations (A= Rb, Tl, Ba). The regular MX_4^{2-} tetrahedra (T_d) coordinate via the triangular faces (facial ligation), while the flattened MCl_4^{2-} tetrahedra (D_{2d}) prefer edge ligation. The cryogenic structure of $[(Tl18C6)_4CuBr_4][TlBr_4]_2$ (**1**) confirms solid-state reorientational motion of coordinated 18C6 previously detected in some metal and metal-free host–guest crystals by variable-temperature solid-state ^1H and ^{13}C NMR (*Chem. Abstr.* **1989**, *111*, 56905b). The motions generating the reorientations are very sensitive to the detailed crystal environment; dependence on crystal water and nature of the 3d element is evident. Crystal data: $[(Tl18C6)_4CuBr_4][TlBr_4]_2$ (**1**) cryogenic (115 K), cubic, space group $F23$ with $a = 20.674(3)$ Å, $V = 8837(1)$ Å^3, $Z = 4$, 700 reflections ($I > 3\sigma(I)$), and $R = 0.054$; $[(Tl18C6)_4MnCl_4][TlCl_4]_2$ (**2**), cubic, space group $F23$ with $a = 20.789(2)$ Å, $V = 8985.2(9)$ Å^3, $Z = 4$, 693 reflections ($I > 1\sigma(I)$), and $R = 0.036$; $(Ba18C6)CoCl_4{\cdot}2H_2O$ (**3**), triclinic, space group $P\bar{1}$ with $a = 8.769(1)$ Å, $b = 10.383(2)$ Å, $c = 13.912(1)$ Å, $\alpha = 98.29(1)°$, $\beta = 89.77(1)°$, $\gamma = 113.64(1)°$, $V = 1146.2(6)$ Å^3, $Z = 2$, 6156 reflections ($I > 3\sigma(I)$), and $R = 0.033$; $Rb(15C5)_2TlBr_4$ (**4**), orthorhombic, space group $Cmcm$, with $a = 13.630(1)$ Å, $b = 11.631(1)$ Å, $c = 22.021(1)$ Å, $V = 3491.0(7)$ Å^3, $Z = 4$, 847 reflections ($I > 1\sigma(I)$), and $R = 0.054$.

Introduction

Tetrahalometalate anions, MX_4^{2-} (M = 3d element and X = halogen atom), have been extensively studied structurally,[1–19] spectroscopically,[20–31] and magnetically.[32–41] However, acknowledgment of their coordinative potential came only recently when the formation of $Cu_2Cl_6^{2-}$ and higher oligomeric species was recognized as ligation of $CuCl_4^{2-}$ to $CuCl_2$.[1] The coordinative versatility of MX_4^{2-} was conclusively demonstrated when accumulation of $A18C6^+$ ions (A = Rb or Tl) on the triangular faces of tetrahedral MX_4^{2-} ligands (herein defined as facial ligation) was accomplished.[42,43] The resulting supramolecular species $[(A18C6)_4MX_4][TlX_4]_2{\cdot}nH_2O$[42,43] have unusual cubic

---

⊛ Abstract published in *Advance ACS Abstracts,* July 1, 1994.

(1) Holvorson, K. E.; Patterson, C.; Willet, R. D. *Acta Crystallogr.* **1990**, *B46*, 508 and references therein.

(2) Mali, T. N.; Wade, P. W.; Hancock, R. D. *J. Chem. Soc., Dalton Trans.* **1992**, 67.

(3) Dyrek, K.; Goslar, J.; Hodorowicz, S. A.; Hoffman, S. K.; Oleksyn, B. J.; Weselucha-Birczyñska, A. *Inorg. Chem.* **1987**, *26*, 1481.

(4) Qui, D. Y.; Pelacios, E. *Acta Crystallogr., Sect. C: Cryst. Struct. Commun.* **1990**, *C46*, 1212.

(5) Geiser, U.; Willett, R. D.; Lindbeck, M.; Emerson, K. *J. Am. Chem. Soc.* **1986**, *108*, 1173.

(6) Hasebe, K.; Asahi, T.; Cresi, K. *Acta Crystallogr., Sect. C: Cryst. Struct. Commun.* **1990**, *C46*, 759.

(7) Chandhuri, S.; Bernejee, T.; Roy, P. N.; Bocelli, G.; Deb Purkayastha, M. K. *Acta Crystallogr., Sect. C: Cryst. Struct. Commun.* **1990**, *C46*, 385.

(8) Brassy, C.; Robert, R.; Bachet, B.; Chevalier, R. *Acta Crystallogr.* **1976**, *B32*, 1371.

(9) Smith, D. W. *Coord. Chem. Rev.* **1976**, *21*, 93. Hathaway, B. J. *Coord. Chem. Rev.* **1982**, *41*, 423.

(10) Gill, N. S.; Nyholm, R. S. *J. Chem. Soc.* **1959**, 3997.

(11) Willett, R. D. *Acta Crystallogr., Sect. C: Cryst. Struct. Commun.* **1991**, *C47*, 1083.

(12) Reinen, D.; Friebel, C. *Struct. Bonding (Berlin)* **1979**, *37*, 1.

(13) Bloomquist, D. R.; Willett, R. D. *Acta Crystallogr.* **1981**, *B37*, 1353.

(14) Searle, G. H.; Wang, D.-N.; Larsen, S.; *Acta Chem. Scand.* **1992**, *46*, 38.

(15) Strettsova, N. R.; Belsky, V. K.; Bulychev, D. M.; Kireeva, O. K. *Inorg. Chim. Acta* **1991**, *189*, 111.

(16) Dukhlev, R.; Brown, I. D. *Acta Crystallogr., Sect. C: Cryst. Struct. Commun.* **1989**, *C45*, 697.

(17) Brassy, C.; Robert, R.; Bachet, B.; Chevalier, R. *Acta Crystallogr.* **1976**, *B32*, 1371.

(18) Chen, X.-M.; Mak, T. C. W. *Inorg. Chim. Acta* **1991**, *189*, 3.

(19) Nakayama, H.; Nakayama, N.; Chihara, H. *Bull. Chem. Soc. Jpn.* **1987**, *60*, 99.

(20) Hipps, K. W.; Mazur, U. *J. Am. Chem. Soc.* **1987**, *109*, 3861.

(21) Writon, M.; Ginley, D. *J. Chem. Phys.* **1974**, *4*, 295.

(22) Presser, N.; Ratner, M. A.; Sundheim, B. R. *J. Chem. Phys.* **1978**, *31*, 281.

(23) Buric, I.; Nikolac, K.; Aleksic, A. *Acta Phys. Pol.* **1986**, *A69*, 561.

(24) Marco de Lucas, M. C.; Rodriques, F. *J. Phys. Condens. Matter* **1989**, *1*, 4245.

(25) Cotton, F. A.; Goodgame, D. M. L.; Goodgame, M. *J. Am. Chem. Soc.* **1962**, *84*, 167.

(26) Furlani, C.; Furlani, A. *Inorg. Nucl. Chem.* **1961**, *19*, 51.

(27) Foster, J. J.; Gill, N. S.; *J. Chem. Soc. A* **1968**, 2625.

(28) Deeth, R. J. *J. Chem. Soc., Dalton Trans.* **1990**, 355.

(29) Lohr, L. L.; Lipscomb, W. H. *Inorg. Chem.* **1963**, *2*, 911.

(30) Desjardins, S. R.; Penfield, K. W.; Cohen, S. L.; Musselman, R. J.; Solomon, E. I. *J. Am. Chem. Soc.* **1983**, *105*, 4590.

(31) Figgis, B. N.; Reynolds, P. A. *J. Phys. Chem.* **1990**, *94*, 2211.

(32) Patyal, B. R.; Scott, B. L.; Willett, R. D. *Phys. Rev.* **1990**, *B41*, 1657 and references therein.

(33) Willett, R. D.; Landee, C. P. *J. Appl. Phys.* **1981**, *52*, 2004.

(34) Kopinga, K.; Tinus, A. M. C.; deJonge, W. T. M.; deVries, G. C. *Phys. Rev.* **1987**, *B36*, 5398.

(35) Landee, C. P.; Djili, A.; Mudgett, D. F.; Newhall, M.; Place, H.; Scott, B.; Willett, R. D. *Inorg. Chem.* **1988**, *27*, 620.

(36) Bonner, J. C. *J. Magn. Mater.* **1980**, *15–18*, 1003.

(37) Willett, R. D.; Wong, R. J.; Numata, M. *Inorg. Chem.* **1983**, *22*, 3189.

(38) Willett, R. D.; Place, H.; Middleton, M. *J. Am. Chem. Soc.* **1988**, *110*, 8639.

(39) Grieb, T.; Kieslich, A.; Lindner, J.; Rauschmann, H.; Strobel, K.; Treutmann, W.; Geick, R. *J. Phys. Condens Matter* **1991**, *48*, 9757.

(40) Walisch, R.; Petersson, J.; Schuessler, D.; Kluthe, S.; Trampert, A.; Holzer, K. P. *Ferroelectrics* **1991**, *124*, 151.

(41) Milia, F.; Papavassiliou, G.; Anagnostopoulos, A. *Z. Naturforsch., A: Phys. Sci.* **1992**, *47*, 120.

(42) Kahwa, I. A.; Miller, D.; Mitchell, M.; Fronczek, F. R.; Goodrich, R. G.; Williams, D. J.; O'Mahoney, C. A.; Slawin, A. M. Z.; Ley, S. V.; Groombridge, C. J. *Inorg. Chem.* **1992**, *31*, 3963.

(43) Kahwa, I. A.; Miller, D.; Mitchell, M.; Fronczek, F. R. *Acta Crystallogr., Sect. C: Cryst. Struct. Commun.* **1993**, *49*, 320.

0020-1669/94/1333-4002$04.50/0

Table 1. Crystallographic Data for Complexes 1–4

	1	**2**	**3**	**4**
chem formula	$C_{48}H_{96}O_{24}CuTl_6Br_{12}$	$C_{48}H_{96}O_{24}MnTl_6Cl_{12}$	$C_{12}H_{28}O_8CoBaCl_4$	$C_{20}H_{40}O_{10}RbTlBr_4$
fw	3306.0	2763.9	638.4	1050.0
cryst system	cubic	cubic	triclinic	orthorhombic
space group	*F*23 (No. 196)	*F*23 (No. 196)	$P\bar{1}$ (No. 2)	*Cmcm* (No. 63)
lattice consts				
a, Å	20.674(3)	20.789(2)	8.769(1)	13.630(1)
b, Å			10.383(2)	11.631(1)
c, Å			13.912(1)	22.021(1)
α, deg			98.29(1)	
β, deg			89.77(1)	
γ, deg			113.64(1)	
V, Å^3	8837(1)	8985.2(9)	1146.2(6)	3491.0(7)
temp, K	115	295	297	294
λ, Å (Mo Kα)	0.710 73	0.710 73	0.710 73	0.710 73
ρ_{calc}, g cm^{-3}	2.485	2.043	1.850	1.998
Z	4	4	2	4
abs coeff (μ), cm^{-1}	166.8	113.8	29.3	106.0
R^a	0.054	0.036	0.033	0.054
$R_w{}^b$	0.048	0.041	0.042	0.046

[a] $R = \sum\|F_o| - F_c\|/\sum|F_o|$. [b] $R_w = (\sum w(|F_o| - |F_c|^2/\sum wF_o{}^2)^{1/2}$.

*F*23 structures in which the $MX_4{}^{2-}$ ligands, including $CuCl_4{}^{2-}$ and $CuBr_4{}^{2-}$, occupy perfect T_d sites. The stabilization of T_d $CuX_4{}^{2-}$ species is very unusual because of the expected Jahn–Teller distortion.[44,45] On the other hand, binding of $Ba18C6^{2+}$ cations by $CuCl_4{}^{2-}$ ligands is inefficient and features bidentate coordination to $Ba18C6^{2+}$ by the edge of the flattened $CuCl_4{}^{2-}$ tetrahedron (D_{2d}) (herein defined as edge ligation).

Although facial and edge ligation by $MX_4{}^{2-}$ ions have been reliably demonstrated[42,43] and are potentially important sources of supramolecular systems with unusual electronic and magnetic properties, key factors influencing their coordination events are yet to be investigated. For example, the thermodynamic factors which contribute to the stabilization of facially coordinated T_d $CuX_4{}^{2-}$ geometry and those mitigating in favor of edge ligation for the smaller and relatively highly charged Ba^{2+} ions are not understood. The molecular recognition processes[46–51] by which accumulation of $A18C6^+$ ions on $MX_4{}^{2-}$ by facial ligation occurs have also not been studied. Further, during the structural studies of $[(Tl18C6)_4CuCl_4][TlCl_4]_2$ and $[(Tl18C6)_4CuCl_4][TlCl_4]_2\cdot 0.25H_2O$[42] we noticed that the 18C6 chelate possessed different rotations about the major symmetry axis in the two crystalline compounds. For metal-free inclusion complexes of 18C6, e.g. $18C6\cdot HClO_4$, reorientations in the solid state have been detected by variable-temperature solid-state ^1H and ^{13}C NMR.[52] Such reorientations could be an important consequence of crown ether flexibility,[53–57] which gives them superior metal ion transport[58] and catalytic[59] properties. However, these 18C6 reorientations have not yet been confirmed crystallographically.

Table 2. Fractional Coordinates and Equivalent Isotropic Thermal Parameters of $[(Tl18C6)_4CuBr_4][TlBr_4]_2$ (**1**) at 115 K with Estimated Standard Deviations in Parentheses

atom	*x*	*y*	*z*	B_{eq},^{a} Å^2
Tl(1)	0.34934(5)	$1 - x$	x	2.163(7)
Tl(2)	0	0	0	0.92(4)
Tl(3)	$^1/_4$	$^1/_4$	$^1/_4$	0.78(4)
Cu	$^3/_4$	$^1/_4$	$^1/_4$	4.2(3)
Br(1)	0.8150(2)	$1 - x$	$1 - x$	10.76(7)
Br(2)	0.0711(1)	x	x	1.58(2)
Br(3)	0.1786(1)	x	x	1.45(2)
O(1)	0.4783(6)	0.6545(7)	0.2875(6)	2.1(3)*
O(4)	0.4048(8)	0.5398(7)	0.2745(8)	2.9(3)*
C(2)	0.495(1)	0.598(1)	0.250(1)	3.0(4)*
C(3)	0.443(1)	0.567(1)	0.223(1)	2.7(5)*
C(5)	0.500(1)	0.747(1)	0.351(1)	2.3(4)*
C(6)	0.529(1)	0.690(1)	0.319(1)	2.3(5)*

[a] Starred *B* values are for atoms that were refined isotropically; B_{iso} is given. $B_{eq} = (8\pi^2/3)\sum_i\sum_j U_{ij}\, a_i{}^* a_j{}^* a_i \cdot a_j$.

For these reasons, we have studied the structures of $[(Tl18C6)_4CuBr_4][TlBr_4]_2$ (**1**)[43] at 115 K and $[(Tl18C6)_4MnCl_4][TlCl_4]_2$ (**2**) at room temperature in order to establish the authenticity of the T_d geometry of $CuX_4{}^{2-}$ ions and the role of Jahn–Teller effects in $[(A18C6)_4CuX_4][TlX_4]_2$ compounds. $MnCl_4{}^{2-}$ is not subject to Jahn–Teller distortion in T_d symmetry; therefore a comparison of structural parameters, particularly the Cl displacement parameters, of $MnCl_4{}^{2-}$ and $CuCl_4{}^{2-}$ should reveal Jahn–Teller contributions which are expected to be greater in the copper species. Reorientations of 18C6 in the solid state were found to occur between 200 and 350 K by CP-MAS NMR;[52] the low-temperature (115 K) structural study was therefore important for confirming these effects. To be sure that edge ligation of $CuCl_4{}^{2-}$ to $Ba18C6^{2+}$ in $(Ba18C6)_2(CuCl_4)_2\cdot 3H_2O$ was not due to Jahn–Teller effects which favor the very common D_{2d} symmetry of $CuCl_4{}^{2-}$, we have prepared and studied the structures of the similar compounds $(Ba18C6)MCl_4\cdot 2H_2O$ (M = Co (**3**), Zn). No Jahn–Teller effects are expected for $ZnCl_4{}^{2-}$ and $CoCl_4{}^{2-}$ anions, and therefore both T_d and D_{2d} geometries are accessible.[14–19] Thus any preference of $Ba18C6^{2+}$ cations for either facial or edge binding should be more reliably discerned for $ZnCl_4{}^{2-}$ and $CoCl_4{}^{2-}$ than $CuCl_4{}^{2-}$.

Finally, the individual components which contribute to the formation of cubic *F*23 structures share important symmetry elements (space group-imposed C_3 symmetry for 18C6, T_d for

---

(44) Rienen, D.; Friebel, C. *Inorg. Chem.* **1984**, *23*, 791.
(45) Rienen, D.; Atanasov, M.; St. Nikolov, G.; Steffen, F. *Inorg. Chem.* **1988**, *27*, 1678.
(46) Lehn, J.-M. *Angew. Chem., Int. Ed. Engl.* **1990**, *29*, 1304 and references therein.
(47) Schnieder, H. J. *Angew. Chem., Int. Ed. Engl.* **1991**, *30*, 1417.
(48) Cram, D. J.; Tanner, M. E.; Knobler, C. B. *J. Am. Chem. Soc.* **1991**, *113*, 7917.
(49) Gokel, G. W. *Chem. Soc. Rev.* **1992**, *21*, 39.
(50) Capagna, S.; Denti, G; Serroni, S.; Ciano, M.; Balzani, V. *Inorg. Chem.* **1991**, *30*, 3728.
(51) Steel, C.; Vögtle, F. *Angew. Chem., Int. Ed. Engl.* **1991**, *30*, 42.
(52) Buchanan, G. W.; Morat, C.; Ratcliffe, C. I.; Ripmeester, J. A. *J. Chem. Soc., Chem. Commun.* **1989**, 1306. Dawes, S. B.; Ward, D. L.; Fussa-Rydel, O.; Huang, R.-H.; Dye, J. L. *Inorg. Chem.* **1989**, *28*, 2132.
(53) Wipff, G.; Weiner, P.; Kollman, P. *J. Am. Chem. Soc.* **1982**, *104*, 3249.
(54) Uiterwijk, J. W. H. M.; Harkema, S.; Van de Waal, B. W.; Göbel, F.; Nibbeling, H. T. M. *J. Chem. Soc., Perkin Trans. 2* **1983**, 1843.
(55) Uiterwijk, J. W. H. M.; Harkema, S.; Feil, D. *J. Chem. Soc., Perkin Trans. 2* **1987**, 721.
(56) Frechette, M.; Butler, I. R.; Hynes, R.; Detellier, C. *Inorg. Chem.* **1992**, *31*, 1650.
(57) Nicholson, D. G.; Sylte, I.; Vasudevan, A. K.; Saethre, L. J. *Acta Chim. Scand.* **1992**, *16*, 358.
(58) Bajaj, A. V.; Poonia, N. S. *Coord. Chem. Rev.* **1988**, *87*, 55.
(59) Roeske, R. W.; Gessellchen, P. D. *Tetrahedron Lett.* **1976**, *38*, 3369.

Table 3. Selected Interatomic Distances and Angles for $[(Tl18C6)_4CuBr_4][TlBr_4]_2$ (**1**) at 115 and 295 K

	distances (Å)			angles (deg)	
atoms	115 K	295 K	atoms	115 K	295 K
Tl(1)–Br(1)	3.5430(8)	3.5629(9)	O(1)–Tl(1)–O(1)	113.7(4)	113.8(5)
Tl(2)–Br(2)	2.547(1)	2.536(2)	O(1)–Tl(1)–O(4)	56.8(4)	55.9(5)
Tl(3)–Br(3)	2.556(1)	2.553(2)	O(1)–Tl(1)–O(4)	57.4(4)	58.2(5)
Cu–Br(1)	2.328(2)	2.311(2)	O(1)–Tl(1)–O(4)	143.8(4)	142.0(5)
Cu–Tl(1)	3.5572(6)	3.5893(8)	O(4)–Tl(1)–O(4)	107.5(4)	105.5(5)
Tl(1)–O(1)	2.96(1)	3.11(2)	O(1)–C(2)–C(3)	114(2)	110(2)
Tl(1)–O(4)	2.99(2)	2.91(2)	O(1)–C(6)–C(5)	109(2)	109(2)
O(1)–C(2)	1.44(3)	1.41(3)	O(4)–C(3)–C(2)	107(2)	109(2)
C(2)–C(3)	1.38(4)	1.47(4)	O(4)–C(5)–C(6)	109(2)	108(2)
C(3)–O(4)	1.45(3)	1.47(3)	C(2)–O(1)–C(6)	119(2)	118(2)
O(4)–C(5)	1.46(3)	1.40(3)	C(3)–O(4)–C(5)	114(2)	108(2)
C(5)–C(6)	1.48(3)	1.49(4)			
C(6)–O(1)	1.43(3)	1.41(3)			

TlX_4^- and MX_4^{2-}). It was thus interesting to determine how changing the nature of the crown would affect molecular recognition processes which assemble the $[(A18C6)_4MX_4][TlX_4]_2$ supramolecular species.[60]

Herein we report the cryogenic structure of **1** and the preparation and room-temperature structures of **2**, **3**, and the sandwich compound $Rb(15C5)_2TlBr_4$ (**4**). The results are the first crystallographic confirmation of solid-state 18C6 reorientations and reveal remarkable coordinative sensitivity of MX_4^{2-} ligands to the detailed nature of cationic species competing for complexation.

Experimental Details

Materials Used. (1) Thallium halides—thallium(I) chloride, thallium(I) bromide, thallium(III) chloride, and thallium(III) bromide—were obtained by neutralizing 99.99% pure Tl_2CO_3 and Tl_2O_3, respectively, with concentrated hydrochloric or hydrobromic acid. The excess acid was evaporated off to yield the crystalline halides. (2) Rubidium chloride and rubidium bromide were prepared by neutralization of 99.99% rubidium carbonate from Aldrich. (3) 18C6 and 15C5 were of 98% purity from Aldrich. (4) Cobalt(II) chloride, copper(II) bromide, copper(II) chloride, manganese(II) chloride, and manganese(II) bromide were of Analar quality of $MX_2{\cdot}nH_2O$ from BDH. (5) Barium chloride dihydrate was of Analar quality from BDH. (6) Cesium bromide was obtained by neutralization of 99.9% cesium carbonate. (7) Potassium bromide was of Spectrosol quality from BDH.

Preparations of the Complexes. $[(Tl18C6)_4CuBr_4][TlBr_4]_2$ (1). The preparation of **1** along with the room-temperature structure was reported recently.[43]

$[(Tl18C6)_4MnCl_4][TlCl_4]_2$ (2). The preparation procedure of **2** is similar to that of $[(Tl18C6)_4CuCl_4][TlCl_4]_2$, which was reported earlier.[42]

$[(Ba18C6)CoCl_4{\cdot}2H_2O$ (3). Crystals of **3** were obtained as large, dark blue parallelepipeds by slowly evaporating off an ethanolic solution of stoichiometric amounts of $BaCl_2{\cdot}2H_2O$, 18C6, and $CoCl_2{\cdot}2H_2O$ in a 50-mL conical flask at 40–43 °C. Yield: ~82%. The preparation of $[(Ba18C6)MCl_4{\cdot}2H_2O]$, (M = Mn, Zn) was accomplished by the same procedure; other temperatures yielded products which lost solvent molecules rapidly, especially for the zinc compound. Anal. Calc for $[(Ba18C6)ZnCl_4{\cdot}2H_2O]$: C, 22.4; Cl, 22.4; H, 4.3. Found: C, 22.44; Cl, 22.08; H, 4.32.

$[Rb(15C5)_2][TlBr_4]$ (4). The preparation of **4** was initially accomplished by evaporating off a methanol/butanol solution containing thallium(III) bromide (0.5 mmol), rubidium(I) bromide (1 mmol), 18C6 (1 mmol), and manganese(II) bromide (0.25 mmol); this mole ratio was designed to produce the anticipated $[(Rb15C5)_4MnBr_4][TlBr_4]_2$ complex. The reactants were first dissolved in methanol (35 mL), starting with 15C5 and RbBr, followed by $TlBr_3$ and $MnBr_2{\cdot}4H_2O$. About 10 mL of *n*-butanol was then introduced, and the resulting solution was evaporated off slowly over 4 days. The crystals were isolated as tabular parallelepipeds in 42% yield. Compound **4** was subsequently prepared from a solution containing RbBr, $TlBr_3$, and 15C5 in a ratio of 1:1:2. The density of the crystals found by the flotation technique using a chloroform/bromoform mixture is 2.00 g/cm³ in both preparations.

$[Cs(18C6)_2][TlBr_4]$. The complex was obtained from a solution containing CsBr, 18C6, $MnBr_2{\cdot}4H_2O$, and $TlBr_3$ in a mole ratio designed to produce $[(Cs18C6)_4MnBr_4][TlBr_4]_2$. Anal. Calc for $[Cs(18C6)_2]$-$[TlBr]$: Br, 26.97; C, 24.32; H, 4.08. Found: Br, 24.86; C, 24.73; H, 4.37.

Crystal Structure Determinations. The essential experimental conditions and resulting crystallographic data are given in Table 1; other details are available as supplementary material. The cryogenic apparatus used for **1** was the Enraf-Nonius N_2 device; the radiation was Mo Kα (0.710 73 Å). Data reduction in all cases included corrections for background and Lorentz and polarization effects, and absorption corrections were based on ψ scans. All structures were solved by the heavy-atom method using heavy atom coordinates of **1** in the room-temperature structure[43] for **1** at 115 K and those from the isomorphous $[(Tl18C6)_4CuCl_4][TlCl_4]_2$[42] for **2** as starting trial refinement models.

For **1**, heavy-atom coordinates were successful, but carbon positions were found by difference maps to be rotated by 26.0° about the 3-fold axis relative to their room-temperature positions (vide infra). Non-hydrogen atoms were refined anisotropically by full-matrix least squares using Enraf-Nonius MolEN programs.[61] For **1**, the 18C6 carbon and oxygen atoms were refined isotropically because attempted anisotropic refinement lead to some nonpositive definite thermal parameters. This is attributed to the near-zero values of the thermal amplitude at cryogenic temperature, as well as the relative unimportance of scattering from C and O atoms in the presence of the very heavy atoms. The hydrogen atoms for **1**–**4** were idealized, assigned isotropic thermal parameters ($B = 1.3B_{eq}$ of attached C), and allowed to ride on parent carbon atoms. The absolute structures for **1** and **2** were determined by *R*-factor tests.

Results and Discussions

Cryogenic Structure of 1. The atomic coordinates for 1 (115 K) and selected interatomic distances and angles are given in Tables 2 and 3, respectively. The "sunrise" conformation typical of the $Tl18C6^+$ cations[42,43] facially bound to T_d $CuBr_4^{2-}$ ligands is shown in Figure 1 for one of the four $Tl18C6^+$ ions. The packing of $[(Tl18C6)_4CuBr_4][TlBr_4]_2$ in the cubic unit cell is the same as that of the room-temperature structure,[43] with the exception of rotation of 18C6 about the C_3 axis. The Br(1)–Cu–Br(1), Br(2)–Tl(2)–Br(2), and Br(3)–Tl(3)–Br(3) bond angles are tetrahedral. The Cu–Br(1) and Tl(1)–Br(1) bond distances at 115 K are within 0.02 Å of those at 295 K. Bond angles about the crown complexed to Tl^+ ions at 115 K and at 295 K agree within their rather large uncertainties. The thermal parameters of the $TlBr_4^-$ ions (average B_{eq} (Å²): Tl (3.60(7)), Br (5.31(3)) at 295 K; Tl (0.85(4)), Br (1.52 (2)) at 115 K) decrease substantially on cooling to 115 K, but those of $CuBr_4^{2-}$ (B_{eq} (Å²): Cu (8.0(4)), Br (12.92(7)) at 295 K; Cu (4.2(3)), Br (10.76(7)) at 115 K)[43] are less sensitive to the 180 K drop in temperature. This indicates that the large values are attributable to disorder of Jahn–Teller distorted tetrahedra rather than librational processes.

The most important change in the structure of **1** on cooling from 295 to 115 K is the orientation of the 18C6 chelate. The

---

(60) Fairman, R. A.; Gallimore, W. A.; Spence, K. V. N.; Kahwa, I. A. *Inorg. Chem.* **1994**, *33*, 823.

(61) Fair, C. K. MolEN, An Interactive Structure Solution Procedure, Enraf-Nonius, Delft, The Netherlands, 1990.

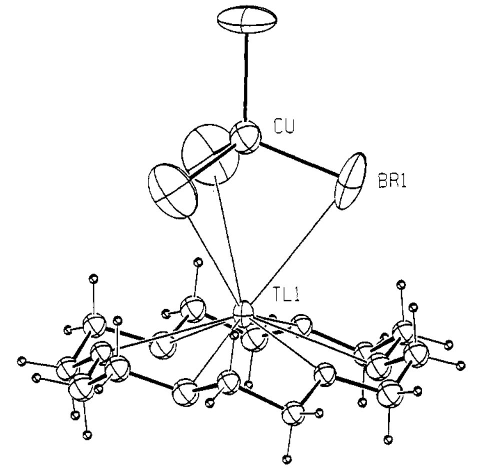

Figure 1. Facial coordination of one of the four Tl18C6$^+$ cations by the tetrahedral (T_d) $CuBr_4^{2-}$ ligandin **1** at 115 K.

18C6 molecule in the cryogenic structure of **1** is rotated by 26.0° about its 3-fold axis relative to the coordinates at 295 K.[43] Macrocycle reorientations in metal-free solid 18C6 host–guest complexes were convincingly detected by variable-temperature solid-state ^{1}H and ^{13}C NMR; transition temperatures of 200–350 K and reorientation activation energies of 31–55 kJ mol^{-1} were measured.[52] These reorientational motions ($T > 230$ K) are probably the cause of the NMR line-narrowing effects observed for the ^{133}Cs and ^{23}Na nuclei in Cs(18C6)$_2$Na observed by Dawes et al.[52] This cryogenic crystallographic study is the first confirmation for 18C6 reorientations in crystalline complexes, and the study further shows that the reorientations do occur in a manner which preserves the crystal structure of the complex and the conformation of the crown as predicted from NMR studies.[52] 18C6 has many possible orientations which have been studied extensively by molecular mechanics.[52–54] The now confirmed ability of 18C6 to adopt different orientations with changing thermal and chemical environment is an important consideration in competitive binding,[56] intricate selective complexation, e.g. in isotopic purification,[62] and functions of ion selective electrodes,[58] as well as crown-mediated catalysis.[59,64] For these reasons, the phenomenon requires further study to determine in detail how guest–host,[47] solvent,[42] and other key molecular interactions affect the progress of these reorientations in both the liquid and solid states.

The relatively greater ease with which 18C6 reorients itself in the solid $HClO_4$·18C6 complex (the transition temperature, 205 K, and activation energy, 31.8 kJ mol^{-1}, were the lowest measured by NMR[52]) prompted us to re-examine the room-temperature structures of the isostructural [(Tl18C6)$_4$CuCl$_4$][TlCl$_4$]$_2$·nH$_2$O (**5**, $n = 0$; **6**, $n = 0.25$)[42] complexes for which the 18C6 orientations are different. The 18C6 chelate in **6** ($T = 297$ K) is rotated by ca. 27.9° about the 3-fold axis of the crown relative to the coordinates of **5** ($T = 297$ K). Actually, the low-temperature (115 K) orientation of the 18C6 in **1** is similar to that found in **6** at 295 K;[42] the orientations of the 18C6 chelate at 295 K in the anhydrous complexes **1**[43] and **5**[42] are similar. The water molecules in **6** occupy positions in the concave sites of Tl18C6$^+$ ions[42] in which the crown–H$_2$O interactions are, expectedly, greatest. It appears that these 18C6–H$_2$O interactions are stabilizing for the low-temperature 18C6 orientation. For $HClO_4$·18C6, however, the strong host–guest H···O(crown) hydrogen bonding interactions appear to stabilize the high-temperature orientation.[52] For **6**, the lone pair on Tl$^+$ which is directed toward the concave faces of the Tl18C6$^+$ complex ion, where the water molecule is also located, could influence the stability of 18C6 orientations and may also interfere with the 18C6–H$_2$O interactions (vide infra).This possibility is being studied using [(Rb18C6)$_4$MX$_4$][TlX$_4$]$_2$·nH$_2$O complexes in which the Rb$^+$ ion has no lone pair.

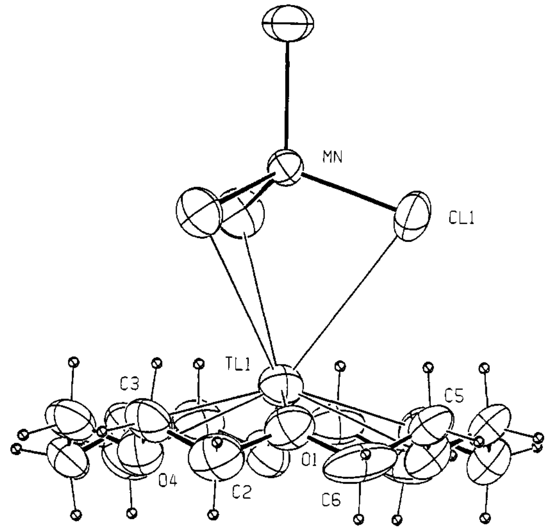

Figure 2. Facial ligation of tetrahedral (T_d) $MnCl_4^{2-}$ anions to Tl18C6$^+$ cations in **2**.

Table 4. Fractional Coordinates and Equivalent Isotropic Thermal Parameters for [(Tl18C6)$_4$MnCl$_4$][TlCl$_4$]$_2$ (**2**)

atom	x	y	z	B_{eq},[a] Å^2
Tl(1)	0.64966(3)	$1 - x$	x	5.157(5)
Tl(2)	1	1	1	5.19(4)
Tl(3)	$^3/_4$	$^3/_4$	$^3/_4$	4.97(4)
Mn	$^1/_4$	$^3/_4$	$^3/_4$	3.7(1)
Cl(1)	0.1852(2)	$1 - x$	$1 - x$	6.22(4)
Cl(2)	0.9331(2)	x	x	8.18(5)
Cl(3)	0.8167(2)	x	x	8.40(6)
O(1)	0.5234(4)	0.3438(5)	0.7121(4)	6.1(2)
O(4)	0.5914(4)	0.4600(5)	0.7244(5)	6.3(3)
C(2)	0.5012(9)	0.4000(7)	0.7483(9)	7.2(3)
C(3)	0.5576(7)	0.4324(7)	0.7732(7)	6.0(4)
C(5)	0.5032(8)	0.2507(8)	0.6450(7)	6.6(3)
C(6)	0.4752(7)	0.310(1)	0.6793(9)	9.0(5)

[a] $B_{eq} = (8\pi^2/3)\Sigma_i\Sigma_j U_{ij}\, a_i^* a_j^* a_i^* a_j$.

Table 5. Selected Interatomic Distances and Angles for [(Tl18C6)$_4$MnCl$_4$][TlCl$_4$]$_2$ (**2**)

	Distances (Å)		
Tl(1)–Cl(1)	3.5885(7)	O(1)–C(2)	1.46(2)
Tl(2)–Cl(2)	2.408(3)	C(2)–C(3)	1.45(2)
Tl(3)–Cl(3)	2.401(3)	C(3)–O(4)	1.36(2)
Mn–Cl(1)	2.333(2)	O(4)–C(5)	1.45(2)
Mn–Tl(1)	3.6131(3)	C(5)–C(6)	1.53(3)
Tl(1)–O(1)	2.93(1)	C(6)–O(1)	1.40(2)
Tl(1)–O(4)	3.01(1)		
	Angles (deg)		
Cl(1)–Tl(1)–Cl(1)	64.12(7)	O(1)–C(2)–C(3)	107(1)
O(1)–Tl(1)–O(1)	114.7(3)	O(4)–C(3)–C(2)	110(1)
O(1)–Tl(1)–O(4)	56.4(3)	O(4)–C(5)–C(6)	105(1)
O(1)–Tl(1)–O(4)	58.4(3)	O(1)–C(6)–C(5)	111(1)
O(1)–Tl(1)–O(4)	144.6(3)	C(2)–O(1)–C(6)	115(1)
O(4)–Tl(1)–O(4)	107.0(3)	C(3)–O(4)–C(5)	111(1)

Structure of 2. The crystal structure of **2** is cubic $F23$ and is isomorphous with **1**; the accumulation of Tl18C6$^+$ ions on the $MnCl_4^{2-}$ anions through facial ligation to yield [(Tl18C6)$_4$MnCl$_4$]$^{2+}$ complex cations is shown, in part, in Figure 2. The packing of [(Tl18C6)$_4$MnCl$_4$]$^{2+}$ and $TlCl_4^-$ ions in the cubic cell is also isomorphous with that of **5** and **6**.[42,43] Atomic coordinates and selected interatomic distances and angles are given in Tables 4 and 5, respectively. The Mn–Cl distances (2.333(2) Å) are

---

(62) Jepson, B. E.; Clager, M. R.; Green, J. L. *Pure Appl. Chem.* **1993**, *65*, 489.

(63) Zhou, W.; Jiang, B.; Pan, X. *Chin. Chem. Lett.* **1991**, *2*, 505.

(64) Dearden, D. V.; Zhang, H.; Chu, I.-H.; Wong, P.; Chen Q. *Pure Appl. Chem.* **1993**, *65*, 423.

Table 6. Coordinates and Equivalent Isotropic Thermal Parameters for (Ba18C6)$CoCl_4 \cdot 2H_2O$ (3)

atom	*x*	*y*	*z*	B_{eq},[a] Å^2
Ba	0.25871(2)	0.34918(2)	0.23723(1)	1.919(3)
Co	0.14923(4)	0.70321(4)	0.28159(3)	2.288(7)
Cl(1)	0.11824(9)	0.54351(8)	0.38337(6)	2.91(1)
Cl(2)	−0.05018(8)	0.79236(8)	0.28523(6)	2.92(1)
Cl(3)	0.1512(1)	0.57307(8)	0.13567(6)	3.40(2)
Cl(4)	0.4002(1)	0.8899(1)	0.3175(1)	5.19(3)
O(1)	0.4939(2)	0.3568(2)	0.0894(2)	2.62(4)
O(2)	0.1562(3)	0.2377(2)	0.0370(2)	2.73(4)
O(3)	−0.0894(3)	0.1767(2)	0.1698(2)	2.95(5)
O(4)	0.0186(3)	0.1716(2)	0.3541(2)	2.90(5)
O(5)	0.3496(3)	0.3035(2)	0.4239(2)	2.84(4)
O(6)	0.5764(2)	0.3483(2)	0.2805(2)	2.84(5)
C(1)	0.4310(4)	0.2926(4)	−0.0084(3)	3.56(8)
C(2)	0.2752(4)	0.3121(4)	−0.0278(2)	3.40(7)
C(3)	−0.0098(4)	0.2159(4)	0.0097(3)	3.22(7)
C(4)	−0.1238(4)	0.1146(4)	0.0695(3)	3.42(7)
C(5)	−0.1956(4)	0.0819(4)	0.2301(3)	3.94(8)
C(6)	−0.1501(4)	0.1468(4)	0.3337(3)	3.89(7)
C(7)	0.0630(4)	0.2020(4)	0.4561(3)	3.45(7)
C(8)	0.2286(4)	0.1955(4)	0.4694(2)	3.42(7)
C(9)	0.5124(4)	0.3096(4)	0.4416(3)	3.40(7)
C(10)	0.6300(4)	0.4082(4)	0.3807(3)	3.07(7)
C(11)	0.7018(3)	0.4043(3)	0.2145(3)	2.96(6)
C(12)	0.6346(4)	0.3291(3)	0.1149(3)	3.06(6)
O(1W)	0.5191(3)	0.6309(3)	0.2712(2)	4.14(6)
O(2W)	0.2363(3)	0.0731(3)	0.2086(2)	4.22(6)

[a] $B_{eq} = (8\pi^2/3)\Sigma_j\Sigma_j U_{ij}a_i^* a_j^* a_i^* a_j$.

Table 7. Bond Distances (Å) for (Ba18C6)$CoCl_4 \cdot 2H_2O$ (3)

Ba–Cl(1)	3.242(1)	O(2)–C(2)	1.430(4)
Ba–Cl(3)	3.317(1)	O(2)–C(3)	1.424(4)
Ba–O(1)	2.893(2)	O(3)–C(4)	1.429(4)
Ba–O(2)	2.858(2)	O(3)–C(5)	1.427(4)
Ba–O(3)	2.926(2)	O(4)–C(6)	1.418(4)
Ba–O(4)	2.863(2)	O(4)–C(7)	1.429(4)
Ba–O(5)	2.877(2)	O(5)–C(8)	1.424(4)
Ba–O(6)	2.856(2)	O(5)–C(9)	1.424(4)
Ba–O(1W)	2.872(2)	O(6)–C(10)	1.440(4)
Ba–O(2W)	2.763(3)	O(6)–C(11)	1.422(4)
Co–Cl(1)	2.267(1)	C(1)–C(2)	1.490(6)
Co–Cl(2)	2.280(1)	C(3)–C(4)	1.483(5)
Co–Cl(3)	2.275(1)	C(5)–C(6)	1.484(5)
Co–Cl(4)	2.271(1)	C(7)–C(8)	1.494(6)
O(1)–C(1)	1.432(4)	C(9)–C(10)	1.491(5)
O(1)–C(12)	1.431(4)	C(11)–C(12)	1.484(5)

shorter than those usually found in uncoordinated $MnCl_4^{2-}$ ions (2.365 Å).[7,17,18] The main objective of studying compound **2** was to establish whether there were any structural differences between **2** and **5**, especially thermal parameters of $MnCl_4^{2-}$ and $CuCl_4^{2-}$ that could suggest Jahn–Teller distortion in $CuCl_4^{2-}$. The isotropic thermal parameter of the Mn^{2+} ion (3.7) is comparable to that of Cu^{2+} (3.78) whereas that of Cl(1) in $MnCl_4^{2-}$ (6.22) is smaller than those of the $TlCl_4^-$ ions in **2** and is also rather smaller than that found in $CuCl_4^{2-}$ (7.35) observed in **1**. The geometry of $CuCl_4^{2-}$ in $[(A18C6)_4CuCl_4][TlCl_4]_2 \cdot nH_2O$ (A = Tl, Rb) is therefore only approximately T_d; a small static distortion from strict T_d symmetry is present.

The 18C6 macrocycle in **2** is rotated by 28.3° about its 3-fold axis relative to the coordinates of **1**. The resulting 18C6 orientation in **2** is similar to that found in the room-temperature structures of **1** and **5**. It therefore appears that the orientation of 18C6 is sensitive to the size and/or detailed electronic properties of the M^{2+} ion in MCl_4^{2-}, as well as the presence or absence of H_2O in the central cavity. Whereas the exact nature of factors influencing the 18C6 motion in solid complexes is yet to be worked out, it is clear from the structures of **1**, **2**, **5**, and **6**, as well as from previous NMR studies, that the 18C6 ring motions are very sensitive to the detailed crystal environment.

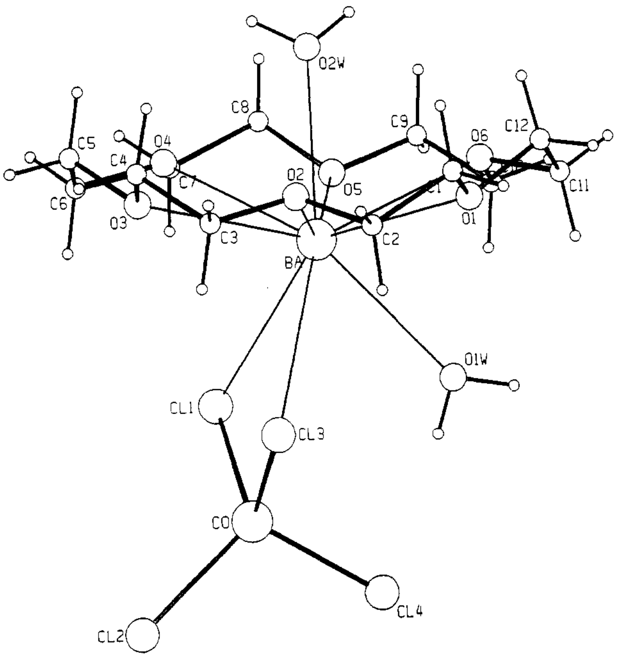

Figure 3. Edge ligation of the distorted tetrahedral (D_{2d}) $CoCl_4^{2-}$ to $(Ba18C6 \cdot 2H_2O)^{2+}$ in **3**.

Table 8. Selected Bond Angles (deg) for (Ba18C6)$CoCl_4 \cdot 2H_2O$ (3)

Cl(1)–Ba–Cl(3)	64.57(2)	O(4)–Ba–O(6)	108.87(7)
Cl(1)–Ba–O(1)	144.01(5)	O(4)–Ba–O(1W)	135.10(8)
Cl(1)–Ba–O(2)	127.03(5)	O(4)–Ba–O(2W)	67.30(8)
Cl(1)–Ba–O(3)	86.38(5)	O(5)–Ba–O(6)	57.68(6)
Cl(1)–Ba–O(4)	71.06(5)	O(5)–Ba–O(1W)	89.16(8)
Cl(1)–Ba–O(5)	78.62(5)	O(5)–Ba–O(2W)	74.78(8)
Cl(1)–Ba–O(6)	120.05(5)	O(6)–Ba–O(1W)	67.66(7)
Cl(1)–Ba–O(1W)	73.34(6)	O(6)–Ba–O(2W)	70.14(7)
Cl(1)–Ba–O(2W)	137.96(6)	O(1W)–Ba–O(2W)	137.06(8)
Cl(3)–Ba–O(1)	90.28(5)	Cl(1)–Co–Cl(2)	115.63(3)
Cl(3)–Ba–O(2)	70.22(5)	Cl(1)–Co–Cl(3)	100.97(3)
Cl(3)–Ba–O(3)	77.03(5)	Cl(1)–Co–Cl(4)	109.21(4)
Cl(3)–Ba–O(4)	116.55(6)	Cl(2)–Co–Cl(3)	113.18(4)
Cl(3)–Ba–O(5)	141.08(5)	Cl(2)–Co–Cl(4)	107.65(4)
Cl(3)–Ba–O(6)	131.83(5)	Cl(3)–Co–Cl(4)	110.04(4)
Cl(3)–Ba–O(1W)	69.22(6)	Ba–Cl(1)–Co	95.20(3)
Cl(3)–Ba–O(2W)	142.40(6)	Ba–Cl(3)–Co	93.07(3)
O(1)–Ba–O(2)	57.51(6)	Cl(1)–O(1)–C(12)	111.0(3)
O(1)–Ba–O(3)	113.92(6)	C(2)–O(2)–C(3)	112.8(3)
O(1)–Ba–O(4)	144.85(7)	C(4)–O(3)–C(5)	111.0(2)
O(1)–Ba–O(5)	115.03(7)	C(6)–O(4)–C(7)	112.5(1)
O(1)–Ba–O(6)	57.83(7)	C(8)–O(5)–C(9)	110.9(3)
O(1)–Ba–O(1W)	73.75(7)	C(10)–O(6)–C(11)	113.5(2)
O(1)–Ba–O(2W)	77.59(8)	O(1)–C(1)–C(2)	108.8(3)
O(2)–Ba–O(3)	57.18(6)	O(2)–C(2)–C(1)	107.1(3)
O(2)–Ba–O(4)	108.49(5)	O(2)–C(3)–C(4)	107.6(3)
O(2)–Ba–O(5)	148.09(7)	O(3)–C(4)–C(3)	109.2(2)
O(2)–Ba–O(6)	110.20(7)	O(3)–C(5)–C(6)	109.4(2)
O(2)–Ba–O(1W)	114.58(8)	O(4)–C(6)–C(5)	108.2(3)
O(2)–Ba–O(2W)	73.31(8)	O(4)–C(7)–C(8)	107.7(3)
O(3)–Ba–O(4)	56.74(7)	O(5)–C(8)–C(7)	108.8(3)
O(3)–Ba–O(5)	114.24(6)	O(5)–C(9)–C(10)	108.8(3)
O(3)–Ba–O(6)	145.98(7)	O(6)–C(10)–C(9)	107.2(2)
O(3)–Ba–O(1W)	145.56(8)	O(6)–C(11)–C(12)	108.2(2)
O(3)–Ba–O(2W)	75.85(8)	O(1)–C(12)–C(11)	109.2(3)
O(4)–Ba–O(5)	57.79(6)		

Structure of 3. The crystal structure of **3**, like that of $(Ba18C6)_2(CuCl_4)_2 \cdot 3H_2O$[42] (**7**), is triclinic space group $P\bar{1}$. However, the two are not isomorphous as they have different H_2O contents. The atomic positions and selected interatomic distances and angles are given in Tables 6-8, respectively; edge ligation and the resulting geometry of the (Ba18C6)$CoCl_4 \cdot 2H_2O$ molecules are shown in Figure 3. The structure of **7** contains two independent molecules, (Ba18C6)$CuCl_4 \cdot 2H_2O$ and (Ba18C6)$CuCl_4 \cdot H_2O$, whereas **3** contains only the dihydrated molecule. Although the $CoCl_4^{2-}$, $ZnCl_4^{2-}$, and $MnCl_4^{2-}$ anions are not subject to Jahn–Teller effects in T_d symmetry, small but significant distortion of these MCl_4^{2-} anions in solid-state structures toward D_{2d} symmetry is frequently

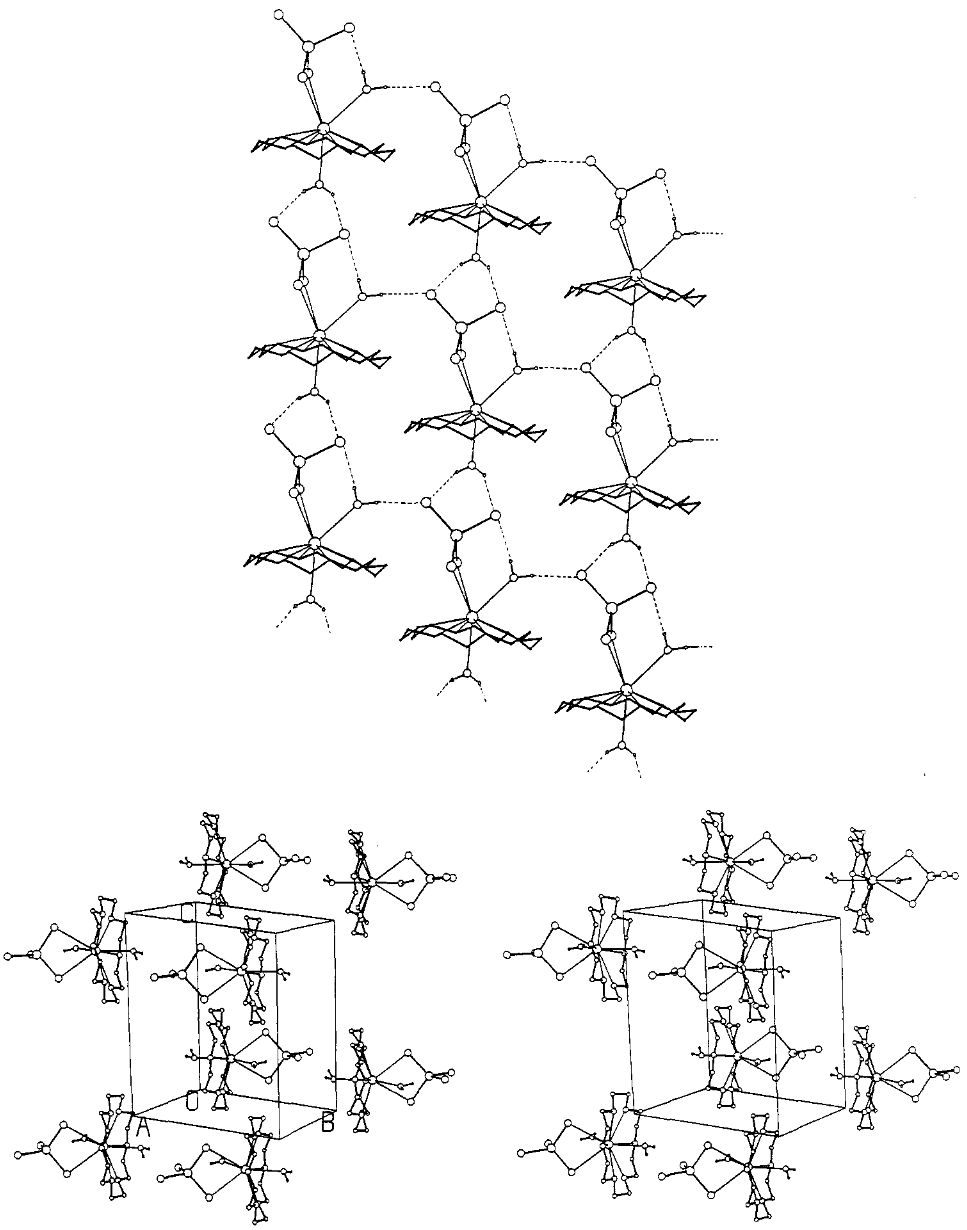

Figure 4. (a) Top: Cutout view of the two-dimensional supramolecular array of [(Ba18C6·2H$_2$O)(CoCl$_4$)] molecules showing the extensive network of Cl···H–O and O···H–O bonds in the crystallographic *a*–*b* plane. There are no H-bonding interactions along the *c* direction. (b) Bottom: Stereoscopic view of the unit cell of [(Ba18C6·2H$_2$O)(CoCl$_4$)] showing the inversion relationship between neighboring *a*–*b* planes.

observed.[14–19] Distortions of uncoordinated MCl$_4^{2-}$ anions are, however, generally small, the Cl–M–Cl bond angles for M = Mn, Co, and Zn tending to be in the range 107–113°.[14–19] The distortions of the Cl–Co–Cl angles (101–115°) from T_d symmetry are significantly larger in 3 and thus reflect the effect of coordination of the CoCl$_4^{2-}$ ligand to the Ba18C6^{2+} cation. Therefore the inability of Ba18C6^{2+} species to undergo facial coordination on triangular faces of CuCl$_4^{2-}$ ligands is not due to Jahn–Teller effects in CuCl$_4^{2-}$. Rather, edge coordination to MCl$_4^{2-}$ ligands under these conditions appears to be preferred by Ba18C6^{2+} cations; the ability of MCl$_4^{2-}$ to adopt D_{2d} symmetry is certainly advantageous. Preference for edge coordination may be due to better competition from a water molecule, O(1W), which shares three of the ten Ba^{2+} coordination sites with MCl$_4^{2-}$ ions (Figure 4). O–H···Cl hydrogen bonding is a source of thermodynamic stability; the structure of 3 features a two-dimensional supramolecular array of O–H···Cl bonds. The O(1W) water molecule forms an intramolecular hydrogen bond to Cl(4) (3.237(3) Å) and an intermolecular hydrogen bond to Cl(2) (3.457(2) Å). The O(2W) water molecule makes intermolecular hydrogen-bonding contacts to Cl(2) (3.309(3) Å) and Cl(4) (3.200(4) Å) which are responsible for the two-dimensional supramolecular chain assembly of molecules of 3 (Figure 4).

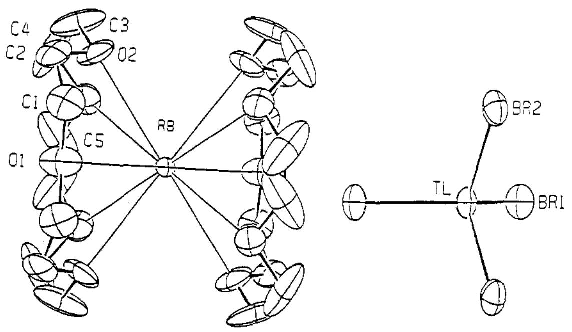

Figure 5. Structure of the Rb(15C5)$_2^+$ sandwich complex in 4.

Preliminary structural results show, however, that the preparation of cubic *F*23 [(K18C6)$_4$MBr$_4$][TlBr$_4$]$_2$·*n*S and [(Ba18C6X)$_4$MnBr$_4$][TlBr$_4$]$_2$·*n*S (where X$^-$ is as yet undetermined and s = solvent molecule) has been accomplished. It is therefore possible that Br···H–O hydrogen bonds are not strong

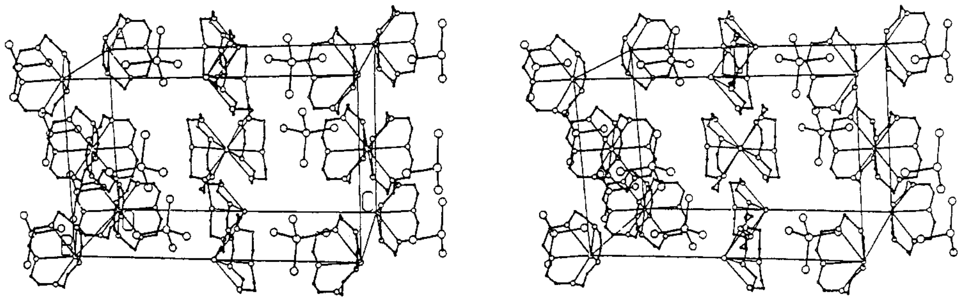

Figure 6. Stereoscopic view of the unit cell of **4** showing the zigzag array of $Rb(15C5)_2^+$ and $TlBr_4^-$ ions.

Table 9. Coordinates and Equivalent Isotropic Thermal Parameters for $Rb(15C5)_2TlBr_4$ (**4**)

atom	*x*	*y*	*z*	B_{eq},[a] Å^2
Tl	0	0.42940(8)	$^1/_4$	7.99(3)
Rb	0	0	0	5.07(5)
Br(1)	0	0.5560(2)	0.1564(1)	11.28(7)
Br(2)	0.1508(2)	0.2987(2)	$^1/_4$	10.82(7)
O(1)	0	−0.060(1)	0.1362(6)	13.8(5)
O(2)	0.1730(6)	0.0141(9)	0.0841(4)	12.4(3)
O(3)	0.1046(8)	0.2201(6)	0.0291(4)	10.7(3)
C(1)	0.089(1)	−0.1094(9)	0.1497(6)	12.2(4)
C(2)	0.165(1)	−0.022(1)	0.1409(6)	11.7(4)
C(3)	0.222(1)	0.119(1)	0.074(1)	21.7(9)
C(4)	0.179(2)	0.211(1)	0.0757(8)	22.4(7)
C(5)	0.039(2)	0.3114(9)	0.0320(9)	24.7(8)

[a] $B_{eq} = (8\pi^2/3)\sum_i\sum_j U_{ij}a_i^*a_j^*a_i^*a_j$.

Table 10. Selected Interatomic Distances and Angles for $Rb(15C5)_2TlBr_4$ (**4**)

	Distances (Å)		
Tl–Br(1)	2.533(2)	O(2)–C(2)	1.33(2)
Tl–Br(2)	2.557(3)	O(2)–C(3)	1.41(2)
Rb–O(1)	3.08(1)	O(3)–C(4)	1.45(2)
Rb–O(2)	3.00(1)	O(3)–C(5)	1.39(2)
Rb–O(3)	3.00(1)	C(1)–C(2)	1.46(2)
O(1)–C(1)	1.38(2)	C(3)–C(4)	1.22(3)
	Angles (deg)		
Br(1)–Tl–Br(1)	108.9(1)	O(2)–Rb–O(3)	123.5(3)
Br(1)–Tl–Br(2)	110.23(3)	O(2)–Rb–O(3)	78.8(3)
Br(2)–Tl–Br(2)	107.0(1)	O(2)–Rb–O(3)	101.2(3)
O(1)–Rb–O(1)	180	O(3)–Rb–O(3)	180
O(1)–Rb–O(2)	53.9(2)	O(3)–Rb–O(3)	123.3(3)
O(1)–Rb–O(2)	126.1(2)	O(3)–Rb–O(3)	56.7(3)
O(1)–Rb–O(3)	89.1(3)	O(1)–C(1)–C(2)	108(1)
O(1)–Rb–O(3)	90.9(3)	O(2)–C(2)–C(1)	114(1)
O(2)–Rb–O(2)	180	O(2)–C(3)–C(4)	122(2)
O(2)–Rb–O(2)	76.5(2)	O(3)–C(4)–C(3)	113(2)
O(2)–Rb–O(2)	103.5(2)	O(3)–C(5)–C(5)	130(1)
O(2)–Rb–O(3)	56.5(3)		

enough to stabilize the triclinic structure such as that of **3**. Thus formation of cubic *F*23 bromide complexes becomes competitive.

Structure of 4. The reaction mixture intended to yield a $[(Rb15C5)_4MnBr_4][TlBr_4]_2$ complex similar to **1**, **2**, **5**, and **6** instead produced $Rb(15C5)_2TlBr_4$ (**4**), containing the $Rb(15C5)_2^+$ sandwich cation (Figure 5). Atomic coordinates and bond angles and distances are given in Tables 9 and 10, respectively. The $Rb(15C5)_2^+$ ion lies on a crystallographic C_{2h} site, and the $TlBr_4^-$ ion on a crystallographic C_{2v} site. Each ion makes two contacts to give an overall infinite zig-zag array of $[Rb(15C5)_2\cdots TlBr_4]_n$ supramolecular species (Figure 6). The $TlBr_4^-$ lies at an *mm* (C_{2v}) site, while the $Rb(15C5)_2^+$ sandwich lies at a *2/m* (C_{2h}) site. The 15C5 group lies on a mirror plane; its high thermal parameters, particularly for the C atoms, are probably indicative of disorder typical of such sandwich complexes.[52]

Competing recognition of $Rb15C5^+$ by the divalent $MnBr_4^{2-}$ ions under the preparative conditions used here for **4** appears to be unfavorable. Complexes isolated in the presence of MX_4^{2-} as sole counteranions are under study. The propensity of the 15C5 cavity to form sandwich compounds is well established, especially that of benzo-15-crown-5;[57,58] even a $Na_2(15C5)_3^{2+}$ club sandwich[67] has been reported. In gas-phase reactions, formation of alkali metal sandwich compounds by the cavity of 15C5 is also predominant.[64,65] But rather few solid rubidium complexes featuring sandwich complexation have been isolated for the 15C5 molecule; the $Rb(15C5)_2^+$ species has only been reported in a pair of crystalline complexes with the unusual Na^- and Rb^- counteranions.[68]

Conclusion

In conclusion, the solid-state 18C6 reorientational motions previously[52] detected by solid-state NMR in metal and metal-free host–guest complexes of 18C6 are general and have now been confirmed crystallographically by a cryogenic study of **1**. But the factors influencing those reorientational motions are still very poorly understood. Facial and edge ligations by MX_4^{2-} appear to be selective and rather specific processes which are sensitive to the detailed nature of cations competing for complexation. For facial ligation, it seems, the metal ion should be large enough to form a sunrise conformation[42] with the crown ether; this condition is fulfilled for 18C6 and M^+ with M = K, Rb, Tl, and BaX. For 15C5, Rb^+ rises too high above the crown to make stable interactions and therefore binding of an extra crown to form a $Rb(15C5)_2^+$ sandwich is preferred. These conclusions were confirmed by studying the $18C6–Cs^+$ system; the synthetic experiment designed for $[(Cs18C6)_4MnBr_4][TlBr_4]_2$ instead produced the sandwich complex $Cs(18C6)_2TlBr_4$ (see Experimental Section).

Acknowledgment. We thank the Department of Chemistry and the Research and Publications Committee, University of the West Indies, for a postgraduate demonstratorship to NSF and for financial support, respectively.

Supplementary Material Available: Tables giving crystal data and details of the structure determinations, hydrogen atom coordinates, all bond distances and angles, and anistropic thermal parameters (18 pages). Ordering information is given on any current masthead page. Structure factor tables are available on request from the authors.

---

(65) Zhang, H.; Chu, I.-H.; Leming, S.; Dearden, D. *J. Am. Chem. Soc.* **1991**, *113*, 7415.

(66) Desiraju, G. R. *Acc. Chem. Res.* **1991**, *24*, 290.

(67) Getman, T. D.; Knobler, C. B.; Hawthorne, M. F. *Inorg. Chem.* **1992**, *31*, 101.

(68) Ward, D. L.; Huang, R-H.; Dye, J. L. *Acta Crystallogr., Sect. C: Cryst. Struct. Commun.* **1990**, *C46*, 1838.